Optics Communications 485 (2021) 126763

Contents lists available at ScienceDirect

Optics Communications

journal homepage: www.elsevier.com/locate/optcom

Polarization control of the high-order harmonics generated from molecules by the carrier envelope phase of few-cycle laser field

Meiyan Qin [a], Feng Wang [a], Kai Liu [a], Zhe Wang [a], Xiaofan Zhang [a], Qing Liao [a,*], Xiaosong Zhu [b,**]

[a] Laboratory for Optical Information Technology, Wuhan Institute of Technology, Wuhan 430205, China
[b] Wuhan National Laboratory for Optoelectronics and School of Physics, Huazhong University of Science and Technology, Wuhan 430074, China

ARTICLE INFO

MSC:
00-01
99-00

Keywords:
Few-cycle circularly polarized laser field
Carrier envelop phase(CEP)
High-order harmonic generation

ABSTRACT

Polarization state of high-order harmonic generation from molecules with few-cycle circularly polarized laser field is investigated. It is found that by controlling the carrier envelope phase (CEP) of the few-cycle driving field, the high-order harmonics with arbitrary polarization state ranging from nearly left circular polarization through linear polarization to nearly right circular polarization can be generated. Moreover, the degree of circular polarization (DCP) of the harmonics changes periodically with the CEP of the driving field. The corresponding period depends on the molecular symmetry. Our results provide a method to control the harmonic polarization with the CEP of few-cycle circularly polarized laser field, which will benefit the generation of isolated attosecond pulses with tunable polarization.

1. Introduction

The rapid development of attosecond physics including the subjects of high-order harmonic generation [1–7], strong field ionization [8–11], target excitation [12], etc., has allowed us to probe ultrafast dynamics in atoms and molecules with attosecond and Ångström resolutions. Since the first demonstrations of circularly polarized harmonics [13,14], the generation and polarization control of nonlinearly polarized extreme ultraviolet and X-ray beams have been a hot topic, due to the ability to study the structural, electronic and magnetic properties of materials in real time. For example, ultrafast circularly polarized pulse can be used to study ultrafast chiral-specific dynamics in molecules and X-ray magnetic circular dichroism spectroscopy [15–18].

In previous works, several methods have been proposed to generate nonlinearly polarized XUV beams based on high-order harmonic generation, which results from the highly nonlinear process induced in a gas medium by an intense femtosecond laser field [19,20]. It has been shown that the nonlinearly polarized harmonics can be generated by using a nonlinearly polarized driving laser [21,22]. In particular, the molecular targets have been widely considered, because the harmonic efficiency driven by circularly polarized fields can be significantly enhanced compared with atomic targets [23–25]. In [26–28], nonlinearly polarized high-order harmonics generated from pre-aligned molecules has also been investigated. Recently, there are several reports of the generation of highly elliptically polarized high-order harmonics using two-color laser field. Some of them use the orthogonal-polarization scheme [17]. Some of them use the bi-chromatic counter-rotating circularly-polarized laser pulses [14,18]. More recently, the polarization property of high-order harmonics by bi-elliptical orthogonally polarized two-color fields were systematically analyzed for atoms [29] and for molecules [30]. Besides of the generation of nonlinearly polarized high-order harmonics, researchers also devote effort to controlling the harmonic polarization, because the polarization control can provide additional degree of freedom for studying and controlling the ultrafast dynamics [31]. Moreover, as a fundamental property of light, it is of great significance to study the light–matter interaction with varying polarization states in the EUV and X-ray spectral range. In [32–34], the authors demonstrated that by using bichromatic circularly polarized laser fields, one can achieve tunable polarization in high-harmonic generation. More recently, it was reported that polarization control of isolated high-harmonic pulses can be achieved by using non-collinear counter-rotating few-cycle driving pulses [35]. Whereas, the harmonic polarization control by the carrier envelope phase (CEP) of a circularly polarized few-cycle laser pulse is seldom investigated. Because the use of few-cycle laser pulse is beneficial for the emission of bright beams and isolated attosecond pulses, the harmonic polarization control via the CEP of driving field gets a distinct importance.

In this paper, we investigate the polarization property of the harmonics driven by a few-cycle circularly polarized laser field. Considering the low efficiency of the harmonics driven by circularly polarized laser field, the molecular target is used. Besides, the few-cycle driving field can further improve the harmonic efficiency, due to the large gradient of the electric field amplitude [36]. It is found that by controlling

* Corresponding author.
** Corresponding author.
E-mail addresses: liaoqing@wit.edu.cn (Q. Liao), zhuxiaosong@hust.edu.cn (X. Zhu).

https://doi.org/10.1016/j.optcom.2021.126763
Received 17 October 2020; Received in revised form 14 December 2020; Accepted 2 January 2021
Available online 5 January 2021
0030-4018/© 2021 Elsevier B.V. All rights reserved.

the carrier envelope phase (CEP) of the driving field, the polarization state of the harmonics can be continuously modulated in a broad range of the polarization state. For example, the degree of circular polarization (DCP) of the 21st order harmonics from N_2 molecule can be tuned from −0.98 through 0.0 to 0.96, i.e. from nearly left circular polarization through linear polarization to nearly right circular polarization. We also investigate the dependence of the harmonic DCP on the CEP of the driving pulse for N_2, CO_2, CO, and He. For all the targets considered here, the DCP of the harmonics changes periodically with the CEP of the driving field. The corresponding period depends on the target symmetry. Both N_2 and CO_2 molecules possess central symmetry. Correspondingly, the harmonic DCP for the two molecules have the same period π. The CO molecule is asymmetric molecule. The corresponding period is 2π. The He atom possesses spherical symmetry and the harmonic DCP is insensitive to the change of the CEP of the driving field. Obviously, the periodicity of the harmonic DCP depends on the target symmetry. Our results provide a method to control the harmonic polarization with the CEP of circularly polarized few-cycle laser field.

2. Theoretical model

In this work, the high-order harmonic generation with a circularly polarized few-cycle laser field is simulated by numerically solving a two-dimensional single-active-electron (SAE) time-dependent schrödinger equation (TDSE)(atomic units are used throughout this paper unless otherwise stated):

$$i\frac{\partial}{\partial t}\Psi(\mathbf{r},t) = \hat{H}(\mathbf{r},t)\Psi(\mathbf{r},t). \tag{1}$$

The Hamiltonian reads

$$\hat{H}(\mathbf{r},t) = -\frac{1}{2}\nabla^2 + V(\mathbf{r}) + \mathbf{r}\cdot\mathbf{E}(t). \tag{2}$$

$\mathbf{E}(t)$ is the electric field and $V(\mathbf{r})$ is the model potential of the target. For the molecular target, we employ the SAE soft-core potential in the form of [37,38]

$$V(\mathbf{r}) = -\sum_j \frac{Z_j^{\infty} + (Z_j^0 - Z_j^{\infty})\exp(-\mathbf{r}_j^2/\sigma_j^2)}{\sqrt{\mathbf{r}_j^2 + b_j^2}}, \tag{3}$$

The subscript $j = 1, \ldots, N$ labels the nuclei at fixed positions $\boldsymbol{\rho}_j$ and $\mathbf{r}_j = \mathbf{r} - \boldsymbol{\rho}_j$. The numerator $Z_j^{\infty} + (Z_j^0 - Z_j^{\infty})\exp(-\mathbf{r}_j^2/\sigma_j^2)$ is the position-dependent screened effective charge for the jth nucleus, where Z_j^{∞} denotes the effective nuclear charge of the nucleus j as seen by an electron at infinite distance and Z_j^0 is the bare charge of nucleus j. Parameter σ_j characterizes the decrease of the effective charge with the increase of the distance to the nucleus. b_j is the soft-core parameter. For the simulations of CO_2 and N_2, the values of the parameters are the same as in [37]. As for the CO molecule, the parameters are the same as in [38]. All these parameters are listed in Table 1.

For the atomic target, the SAE soft-core potential is in the form [39]

$$V(\mathbf{r}) = -\frac{1}{\sqrt{\mathbf{r}^2 + b^2}}, \tag{4}$$

with b the soft-core parameter. To simulate the He atom, the value of b is chosen as 0.27 to obtain an ionization potential of 24.26 eV.

The TDSE is solved using the split-operator method [40]. By the imaginary-time propagation, the initial state is obtained. Then starting from this initial state, the time-dependent wavefunction is calculated by real-time propagation. According to the Ehrenfest theorem [41], the time-dependent dipole acceleration is calculated by

$$\mathbf{A}(t) = -\langle\Psi(\mathbf{r},t)|\nabla V(\mathbf{r}) + \mathbf{E}(t)|\Psi(\mathbf{r},t)\rangle. \tag{5}$$

After obtaining the dipole acceleration, the harmonic spectrum is given by the Fourier transform of the time-dependent dipole acceleration,

$$a_q = \int A_q(t)\exp(-in\omega_0 t)dt, \quad q = x,\ y. \tag{6}$$

Table 1
Values of all parameters used for soft-core potentials of CO_2, N_2, and CO [37,38].

Molecule	CO_2			N_2		CO	
Nucleus	O	C	O	N	N	C	O
$b_j(a.u.)$	1.0	1.0	1.0	1.2	1.2	0.5	0.5
$\sigma_j^2(a.u.)$	0.577	0.750	0.577	0.700	0.700	0.573	0.573
Z_j^0	8	6	8	7	7	4	6
Z_j^{∞}	0.173	0.654	0.173	0.500	0.500	0.4	0.6

The intensity of left- and right-polarized harmonic components can be obtained by

$$D_{\pm} = |a_{\pm}|^2, \tag{7}$$

where $a_{\pm} = \frac{1}{\sqrt{2}}(a_x \pm ia_y)$. The polarization state of high harmonics can be characterized by the degree of circular polarization (DCP) [42],

$$\zeta = \frac{D_+ - D_-}{D_+ + D_-}, \tag{8}$$

which can be obtained from the intensity measurements. The ellipticity ϵ has a one-to-one correspondence with the DCP as $\zeta = \frac{2\epsilon}{1+\epsilon^2}$. The two parameters both vary in the interval from −1 to 1 and have the same sign.

The rotation direction of the electric field can be quantitatively described by the helicity, which is defined as

$$h = sgn(\epsilon) = sgn(\zeta). \tag{9}$$

The helicity h takes the values -1 and +1, indicating the two opposite rotation directions.

3. Result and discussion

In our simulation, we use a circularly polarized few-cycle laser field, which propagates along the z axis. Then the x and y components of the electric field are respectively given by

$$E_x(t) = \frac{E_0}{\sqrt{2}}\sin^2(\frac{\pi t}{T})\sin(\omega t + \varphi) \tag{10}$$

$$E_y(t) = \frac{E_0}{\sqrt{2}}\sin^2(\frac{\pi t}{T})\cos(\omega t + \varphi) \tag{11}$$

Here, $E_0 = \sqrt{\frac{8\pi I_0}{c}}$ is the field amplitude corresponding to the intensity I_0. φ represents the carrier envelope phase of the driving field. T is the total pulse duration. In Fig. 1, high-order harmonic spectra generated from N_2 aligned at 0 degree (a), CO_2 aligned at 30 degree (b) and CO aligned at 0 degree (c) by circularly polarized few-cycle laser field are presented by blue solid lines, respectively. The intensities of the driving fields are 3.0×10^{14} W/cm^2 for N_2 molecule, 1.0×10^{14} W/cm^2 for CO_2 and CO molecules. The wavelength and the total pulse duration of the driving field for all the cases are 800 nm and 3 optical cycles, respectively. For comparison, the harmonic spectra generated from N_2, CO_2 and CO molecules by linearly polarized laser field with the same intensity of the circularly polarized driving fields are also presented by red dotted lines in Fig. 1. For each molecule, the parameters of linearly polarized laser field are the same as those of circularly polarized laser field. As shown in Fig. 1, the harmonic intensities driven by circularly polarized laser field are about 4-order lower, 3-order lower, and 2-order lower than those driven by linearly polarized laser field for N_2, CO_2 and CO molecules, respectively. The harmonic cutoff is also lower in the case of circularly polarized laser pulse, which is around $I_p + 2.0U_p$ [23,36]. While the harmonic cutoff locates around $I_p + 3.17U_p$ [19,20] for linearly polarized laser pulse, where I_p is the ionization energy of the target and U_p is the ponderomotive energy. Although the harmonic intensity driven by circularly polarized laser pulse is lower than that driven by linearly polarized laser pulse, it is possible to be observed in experiment when a few-cycle laser pulse and molecular targets are used, as shown in Fig. 1.

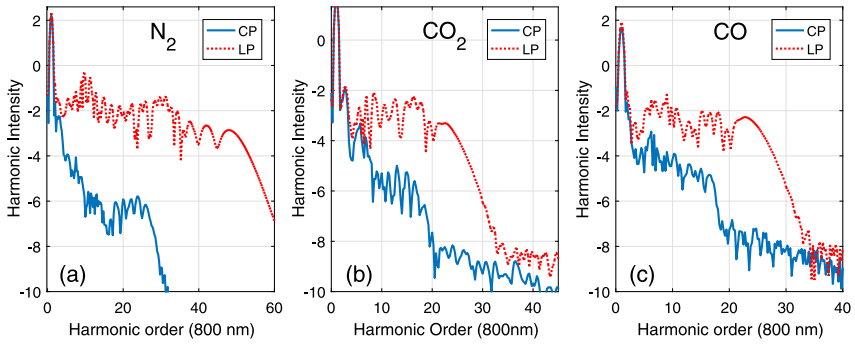

Fig. 1. Harmonic spectra generated from N_2 aligned at 0 degree (a), CO_2 aligned at 30 degree (b), and CO aligned at 0 degree (c) by circularly polarized (blue solid lines) and linearly polarized (red dotted lines) few-cycle laser fields. For each molecule, the laser parameters of circularly polarized laser field and linearly polarized laser field are the same. The intensities of the driving fields are 3.0×10^{14} W/cm^2 for N_2 and 1.0×10^{14} W/cm^2 for CO_2 and CO molecules. The wavelength is $\lambda = 800$ nm and the total pulse duration is 3 optical cycles for all the cases.

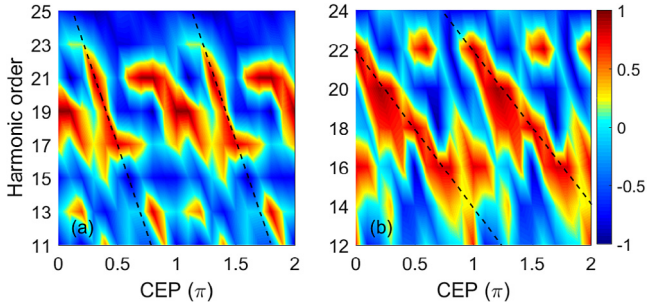

Fig. 2. Pcolor plots with smoothed color of the DCP of the harmonics generated from N_2 molecule aligned at 0 degree as a function of the CEP of the driving field and the harmonic order. The color map of Figs. 1(a) and 1(b) represent the DCP of the odd-order harmonics and the even-order harmonics, respectively. The driving field is a circularly polarized few-cycle laser field with intensity $I_0 = 3.0\times10^{14}$ W/cm^2 and wavelength $\lambda = 800$ nm. The total pulse duration is 3 optical cycles.

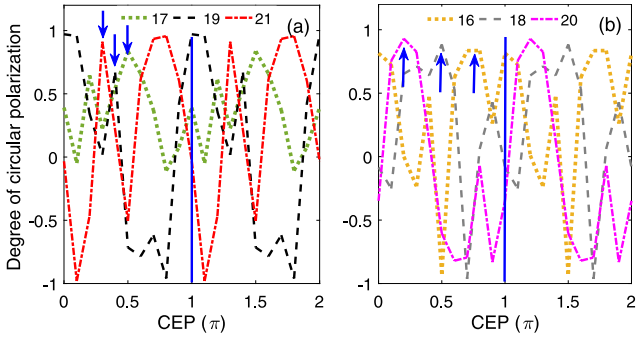

Fig. 3. The DCP of the odd (Panel a) and even (Panel b) order harmonics as a function of the CEP of driving field, extracted from Fig. 1. The 17th, 19th, and 21st order harmonics are presented in Fig. 2(a). The 16th, 18th, and 20th order harmonics are presented in Fig. 2(b). The blue arrows indicate the local peaks of the DCP of the harmonics. The blue solid lines indicate the period of the harmonic DCP.

We first investigate the polarization property of the high-order harmonics generated from N_2 molecule with the circularly polarized few-cycle laser field. The laser parameters are the same as those for Fig. 1(a). In Figs. 2(a) and 2(b), pcolor plots with smoothed color of the DCP of the harmonics are presented for the odd-order harmonics and the even-order harmonics, respectively. The horizontal axis stands for the CEP of the driving pulse and the vertical axis stands for the harmonic order. The color bar represent the value of the harmonic DCP. From these two figures, one can see that the distribution of the harmonic DCP present three interesting features for both the odd and even order harmonics. First, the DCP of the harmonics can vary approximately from −1 to 1. This means that the harmonics can be tuned from left circular polarization through linear polarization to right circular polarization by changing the CEP of the driving field. Second, the DCP of all the harmonics varies periodically with the CEP of the driving field. The corresponding period is π for all the harmonics, which is different from the 2π period of the driving field. Third, the harmonic order where the peak value of the DCP locates linearly varies with the CEP of the driving pulse, as shown by the black dashed lines in Figs. 2(a) and 2(b) for the odd and even order harmonics, respectively. The major difference is that the slope of the straight line for the odd harmonics is larger than that for the even order harmonics.

For clarity, the DCP as a function of the CEP of driving field for specific odd and even order harmonics are presented in Figs. 3(a) and 3(b), respectively. The green dotted, black dashed, and red dash-dotted lines in Fig. 3(a) represent the 17th, 19th, 21st order harmonics, respectively. The yellow dotted, gray dashed, and pink dash-dotted lines in Fig. 3(b) represent the 16th, 18th, 20th order harmonics, respectively. As shown in Fig. 3 for both odd and even order harmonics, the DCP of the harmonics present a periodic behavior. The corresponding period is π for all the harmonics. When the CEP of the driving field varies from 0 to π, the DCP of the 21st order harmonics present an oscillation behavior. The minimum value −0.98 of the DCP is achieved at the CEP of 0.1π, which corresponds to the nearly left circular polarization. The maximum value 0.96 of the DCP is achieved at the CEP of 0.8π, which corresponds to the nearly right circular polarization. By controlling the CEP of the driving field, the DCP of the 21st order harmonics can reach the values among [-0.98,0.96]. Correspondingly, the 21st order harmonics can be tuned among the polarization states from the nearly left circular polarization through the linear polarization to the nearly right circular polarization, as shown by the red dash-dotted line in Fig. 3(a). As for the 19th order harmonics, the harmonic DCP can be tuned among the values from −0.96 to 0.97. It means that the polarization state of the 19th order harmonics can also be continuously tuned between nearly left circular polarization and nearly right circular polarization. While for the 17th order harmonics, the DCP range that can be tuned is [-0.11,0.84], as shown by the green dotted line in Fig. 3(a). The DCP of the even order harmonics in Fig. 3(b) can also be tuned by changing the CEP of the driving field. The modulation ranges of the harmonic DCP are from 0.836 to −0.924 for the 16th order harmonics, from 0.884 to −0.924 for the 18th order harmonics, and from 0.93 to −0.82 for the 20th order harmonics, respectively. In Fig. 3(a) and (b), the blue arrows indicate the local peaks of the DCP of the harmonics. The intervals between two nearby peaks of the harmonic DCP are equal in both cases of odd-order and even-order harmonics. For the odd order harmonics, this interval is smaller than those for the even order harmonics, which corresponds to the third feature observed in Fig. 2. From the above discussion, one can see that the polarization

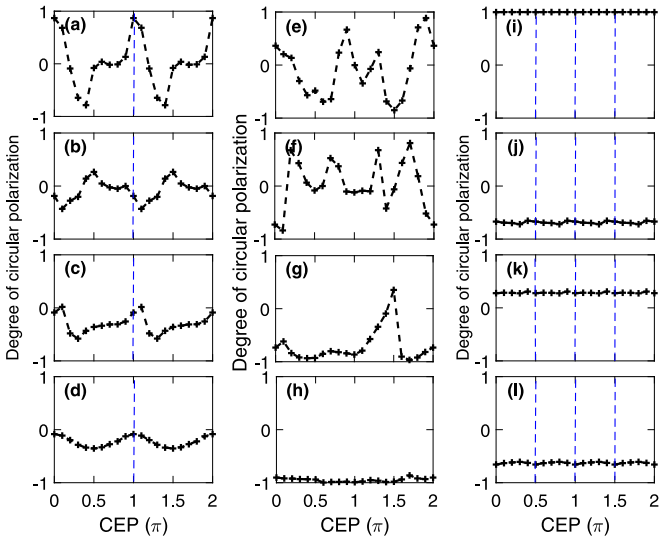

Fig. 4. The DCP of the 11th, 13th, 15th, and 17th order harmonics generated from CO_2 molecule aligned at 0 degree (a–d), CO molecule aligned at 0 degree (e–h), and He atom (i–l) as a function of the CEP of driving field. The first, second, third, and fourth rows correspond to the 11th, 13th, 15th, and 17th order harmonics, respectively. The intensity of the driving field is $I_0 = 1.0 \times 10^{14}$ W/cm^2. Other parameters of the driving field are the same to those used in Fig. 2.

state of the harmonics considered here can be tuned in a broad range, by changing the CEP of the driving field.

We also investigate the dependence of the harmonic DCP on the CEP of the driving pulse for CO_2 molecule, CO molecule, and He atom. The results are presented in Fig. 4. The first, second, and third columns of Fig. 4 correspond to the results of CO_2 molecule, CO molecule, and He atom, respectively. Because the DCP of the even order harmonics present similar features to that of the odd order harmonics, we just consider the odd order harmonics here. They are 11th, 13th, 15th, and 17th order harmonics and are presented in the first, second, third, and fourth rows of Fig. 4, respectively. The intensity of the driving field is $I_0 = 1.0 \times 10^{14}$ W/cm^2. Other parameters of the driving field are the same as those used in Fig. 2. For the case of CO_2 molecule shown in the first column, the DCP of the 11th order harmonics can be tuned among the values from −0.79 to 0.87. This corresponds to a broad range of the polarization state. When the harmonic order increases, the range that the harmonic DCP can be tuned decreases. For the 13th order harmonics, the harmonic DCP can be tuned among the values from −0.43 to 0.27. As for the 15th and 17th order harmonics, the range that the harmonic DCP can be tuned is from 0.58 to 0.01 and from −0.35 to −0.08, respectively. It is obvious that the harmonic DCP varies periodically with the CEP of the driving field, as shown in Fig. 4(a)-4(d) for CO_2 molecule. The corresponding period is π, which is the same as that for N_2 molecule. In the case of CO molecule, the ranges that the harmonic DCP can be tuned are from −0.85 to 0.87 for the 11th order harmonics, from −0.84 to 0.81 for the 13th order harmonics, from −0.97 to 0.35 for the 15th order harmonics. While for the 17th order harmonics, the harmonic DCP present tiny variation when the CEP of the driving field changes, as shown in Fig. 4(h). The period of the harmonic DCP are 2π for all the harmonics, which is the same to the driving field. In the case of He atom, the harmonic DCP are the same for all the CEP of the driving field, as shown in Fig. 4(i)–(l). The tiny deviations result from the non-isotropic spatial grid. From the above discussion, one can see that the polarization state of the harmonics generated from CO_2 and CO molecules can also be tuned in a broad range by controlling the CEP of the circularly polarized few-cycle driving field, while for the He atom, the harmonic polarization state cannot be tuned by the change of the CEP of the driving field.

To explain the periodicity observed in the harmonics generated from N_2, CO_2, CO, and He, we perform an analysis of the symmetry of the driving field and the target. In Figs. 5(a)–5(d), the electric field for the CEP of 0.0π, 0.5π, 1.0π, and 1.5π are presented, respectively. As shown in Fig. 5(a)–(d), changing the CEP of the driving field is equivalent to rotating the electric field. For the CEP of 0.0π, the maximum electric field points to the negative direction of the y axis, as indicated by the red dashed arrow in Fig. 5(a). When the CEP of driving field is changed to 0.5π, the electric field is clockwise rotated by 90 degrees with respect to the case of the CEP being 0.0π. Hence, the maximum electric field points to the negative direction of the x axis, as indicated by the red dashed arrow in Fig. 5(b). When the CEP is changed to 1.0π, the electric field is clockwise rotated by 180 degrees with respect to the case of CEP being 0.0π. Similarly, the electric field with CEP $\varphi = 1.5\pi$ is clockwise rotated by 270 degrees with respect to the case of $\varphi = 0.0\pi$.

In Fig. 5(e)–(h), the involved molecular orbital of He, N_2, CO_2, and CO are presented. In the case of CO_2 molecule, it possesses two degenerate highest occupied molecular orbitals (HOMO). Whereas, the harmonic emission is only contributed by the HOMO that lies parallel to the polarization plane of the driving field. This is because the nodal plane of the other degenerate HOMO lies parallel to the polarization plane of the driving field. This will lead to zero dipole moment and no harmonic emission. Hence, only the HOMO that lies parallel to the polarization plane of driving field is involved in the case of CO_2 molecule, as shown in Fig. 5(g). From Fig. 5(e)–(h), one can see that the He atom is spherically symmetric, whereas the N_2 and CO_2 molecules are centrosymmetric. The CO molecule possesses only cylindrical symmetry. For the He target, the responses to the driving field polarized along any direction are the same due to the spherical symmetry. Hence, the harmonics is insensitive to the change of the CEP of driving field. As for the N_2 and CO_2 molecules, the orbitals are centrosymmetric. This means that the orbital is invariant after rotated by 180 degrees. Hence, the responses of N_2 and CO_2 molecules to the driving fields of which the CEP difference is π are the same. Consequently, the period of the harmonic DCP is 1.0π in the cases of the N_2 and CO_2 molecules. As for the CO molecule, it does not possess central symmetry. Hence, the period of the DCP of the harmonics is the same to the driving field, i.e. 2.0π. For the N_2 and CO_2 molecules possessing the same orbital symmetry, the periods of the harmonic DCP for the two molecules are correspondingly the same. For He, N_2(CO_2), and CO molecules possessing different orbital symmetry, the periods of the harmonic DCP for the three molecules are corresponding different. Hence, the molecular orbital symmetry is imprinted in the periodicity of the harmonic DCP as a function of the CEP of the driving field.

Based on the three-step model for high harmonic generation from oriented molecules, the observed harmonic polarization control with the CEP of circularly polarized few-cycle laser field for N_2, CO_2, and CO molecules can be qualitatively explained. As shown in Fig. 5(a)–(d), varying the CEP of the laser field will rotate the two-dimension pattern of the electric field. Correspondingly, the electron trajectory as well as the electron recombination angle with respect to the internuclear axis of molecule are changed by varying the CEP of the laser field. It has been shown that the harmonic polarization depends on the electron recombination angle and the symmetry of molecular orbitals [26,27]. Therefore, the harmonic polarization is controlled by the CEP of the circularly polarized few-cycle laser field for N_2, CO_2, and CO molecules. As for He atom, it possesses spherical symmetry, as shown in Fig. 5(e). Hence, high-order harmonic generation is independent on the electron recombination angle. Consequently, the harmonic polarization state cannot be tuned by the change of the CEP of the driving field.

4. Conclusion

In conclusion, we investigate the dependence of the harmonic DCP on the CEP of circularly polarized few-cycle laser field. It is demonstrated that by controlling the CEP of circularly polarized few-cycle

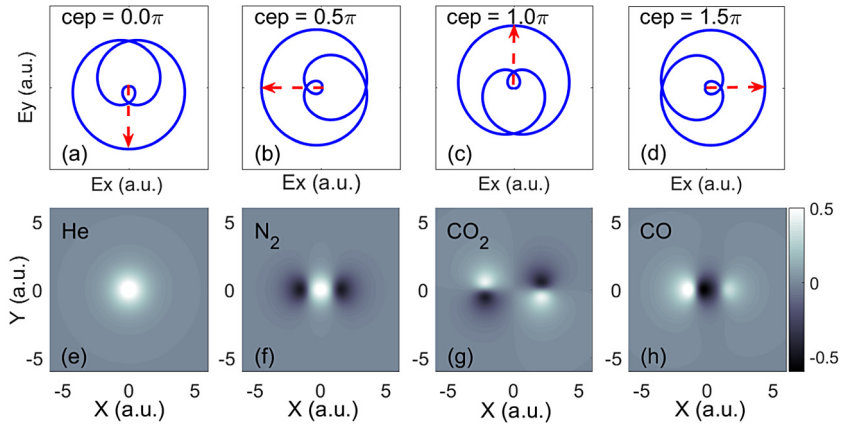

Fig. 5. (a–d) The two-dimensional electric field of the circularly polarized few-cycle laser field with CEP 0.0π, 0.5π, 1.0π, 1.5π, respectively. (e–h) The ground state wavefunction of He, N_2, CO_2, and CO molecules.

driving pulse, the DCP of the harmonics generated from N_2, CO_2, and CO molecules can be tuned in a broad range of the polarization state. The DCP of the harmonics generated from N_2 molecule can be tuned from −0.98 to 0.96, i.e. from nearly left circular polarization through linear polarization to nearly right circular polarization. It is also found that the DCP of the harmonics change periodically with the CEP of the driving field. The corresponding period depends on the target symmetry. If the molecular orbital symmetry is the same, then the period of the harmonic DCP is the same, as for the cases of N_2 and CO_2 molecules. If the molecular orbital symmetry is different, then the period of the harmonic DCP is also different, as the periods of the harmonic DCP for He, N_2 (CO_2), and CO molecules are different. Hence, the degree of the target symmetry is imprinted in the periodicity of the harmonic DCP as a function of the CEP of the driving field. Because the intensity of the driving field we used is relatively low, the macroscopic propagation effect is not significant. Moreover, the macroscopic propagation effect mainly changes the harmonic intensity and has few influences on the harmonic polarization property. Hence, the macroscopic propagation effect does not change our conclusions.

Declaration of competing interest

The authors declare that they have no known competing financial interests or personal relationships that could have appeared to influence the work reported in this paper.

Acknowledgments

This work is supported by National Natural Science Foundation of China (NSFC) (No. 11604248, No. 11674257, No. 11904269, No. 11947096); National College Students' innovation and entrepreneurship training program, China (No. 201810490023); the Program for Distinguished Middle-aged and Young Innovative Research Team in Higher Education of Hubei, China (No. T201806); the Natural Science Foundation of Hubei Province, China under Grants No. 2017CFB150.

References

[1] M. Ferray, A. L'Huillier, X.F. Li, L.A. Lompre, G. Mainfray, C. Manus, Multiple-harmonic conversion of 1064 nm radiation in rare gases, J. Phys. B 21 (1988) L31.

[2] P. Lan, M. Ruhmann, L. He, C. Zhai, F. Wang, X. Zhu, Q. Zhang, Y. Zhou, M. Li, M. Lein, P. Lu, Attosecond probing of nuclear dynamics with trajectory-resolved high-harmonic spectroscopy, Phys. Rev. Lett. 119 (2017) 033201.

[3] L. He, Q. Zhang, P. Lan, W. Cao, X. Zhu, C. Zhai, F. Wang, W. Shi, M. Li, X. Bian, P. Lu, A.D. Bandrauk, Monitoring ultrafast vibrational dynamics of isotopic molecules with frequency modulation of high-order harmonics, Nature Commun. 9 (2018) 1108.

[4] B. Wang, L. He, Y. He, Y. Zhang, R. Shao, P. Lan, P. Lu, All-optical measurement of high-order fractional molecular echoes by high-order harmonic generation, Opt. Express 27 (2019) 30172–30181.

[5] J. Wang, A. Liu, K.-J. Yuan, High-order harmonic generation in aligned molecules by combination of weak XUV and intense IR laser pusles, Opt. Commun. 460 (2020) 125216.

[6] J. Han, J. Wang, Y. Qiao, A. Liu, F. Guo, Y. Yang, Significantly enhanced conversion efficiency of high-order harmonic generation by inducing chirped laser pulse into scheme of spatially inhomogeneous field, Opt. Express 27 (2019) 8768.

[7] Y. Guo, A. Liu, J. Wang, X. Liu, Atomic even-harmonic generation due to symmetry-breaking effects induced by spatially inhomogeneous field, Chin. Phys. B 28 (2019) 094212.

[8] Y. Zhou, O.I. Tolstikhin, T. Morishita, Near-forward rescattering photoelectron holography in strong-field ionization: extraction of the phase of the scattering amplitude, Phys. Rev. Lett. 116 (2016) 173001.

[9] Y. Zhao, Y. Zhou, J. Liang, Z. Zeng, Q. Ke, Y. Liu, M. Li, P. Lu, Frustrated tunnelling ionization in the elliptically polarized strong laser fields, Opt. Express 27 (2018) 21689–21701.

[10] J. Tan, Y. Li, Y. Zhou, M. He, Y. Chen, M. Li, P. Lu, Identifying the contributions of multiple-returning recollision orbits in strong-field above-threshold ionization, Opt. Quant. Electron 50 (2018) 57.

[11] Q. Liao, A.H. Winney, S.K. Lee, Y.F. Lin, P. Adhikari, W. Li, Coulomb-repulsion-assisted double ionization from doubly excited states of argon, Phys. Rev. A 96 (2017) 023401.

[12] H. Niikura, F. Légaré, R. Hasbani, A.D. Bandrauk, M.Y. Ivanov, D.M. Villeneuve, P.B. Corkum, Sub-laser-cycle electron pulses for probing molecular dynamics, Nature 417 (2002) 917.

[13] A. Fleischer, O. Kfir, T. Diskin, P. Sidorenko, O. Cohen, Spin angular momentum and tunable polarization in high-harmonic generation, Nat. Photon. 8 (2014) 543–549.

[14] O. Kfir, P. Grychtol, E. Turgut, R. Knut, D. Zusin, D. Popmintchev, T. Popmintchev, H. Nembach, J.M. Shaw, A. Fleischer, H. Kapteyn, M. Murnane, O. Cohen, Generation of bright phase-matched circularly polarized extreme ultraviolet high harmonics, Nat. Photon. 9 (2015) 99–105.

[15] A.D. Bandrauk, J. Guo, K. Yuan, Circularly polarized attosecond pulse generation and applications to ultrafast magnetism, J. Opt. 19 (2017) 124016.

[16] O. Kfir, S. Zayko, C. Nolte, M. Sivis, M. Möller, B. Hebler, S. Arekapudi, D. Steil, S. Schäfer, M. Albrecht, O. Cohen, S. Mathias, C. Ropers, Nanoscale magnetic imaging using circularly polarized high-harmonic radiation, Sci. Adv. 3 (2017) eaao4641.

[17] G. Lambert, B. Vodungbo, J. Gautier, B. Mahieu, V. Malka, S. Sebban, P. Zeitoun, J. Luning, J. Perron, A. Andreev, S. Stremoukhov, F. Ardana-Lamas, A. Dax, C.P. Hauri, A. Sardinha, M. Fajardo, Towards enabling femtosecond helicity-dependent spectroscopy with high-harmonic sources, Nature Commun. 6 (2015) 6167.

[18] T. Fan, P. Grychtol, R. Knut, C. Hernández-García, D.D. Hickstein, D. Zusin, C. Gentry, F.J. Dollar, C.A. Mancuso, C.W. Hogle, O. Kfir, D. Legut, K. Carva, J.L. Ellis, K.M. Dorney, C. Chen, O.G. Shpyrko, E.E. Fullerton, O. Cohen, P.M. Oppeneer, D.B. Milošević, A. Becker, A.A. Jaroń-Becker, T. Popmintchev, M.M. Murnane, H.C. Kapteyn, Bright circularly polarized soft X-ray high harmonics for X-ray magnetic circular dichroism, Proc. Natl. Acad. Sci. USA 112 (2015) 14206–14211.

[19] P.B. Corkum, Plasma perspective on strong-field multiphoton ionization, Phys. Rev. Lett. 71 (1993) 1994–1997.

[20] M. Lewenstein, P. Balcou, M.Y. Ivanov, A. L'Huillier, P.B. Corkum, Theory of high-harmonic generation by low-frequency laser fields, Phys. Rev. A 49 (1994) 2117–2132.

[21] V.V. Strelkov, A.A. Gonoskov, I.A. Gonoskov, M. Yu. Ryabikin, Origin for ellipticity of high-order harmonics generated in atomic gases and the sublaser-cycle evolution of harmonic polarization, Phys. Rev. Lett. 107 (2011) 043902.
[22] X. Zhu, M. Qin, Q. Zhang, W. Hong, Z. Xu, P. Lu, Role of the Coulomb potential on the ellipticity in atomic high-order harmonics generation, Opt. Express 20 (2012) 16275–16284.
[23] X. Zhu, X. Liu, Y. Li, M. Qin, Q. Zhang, P. Lan, P. Lu, Molecular high-order-harmonic generation due to the recollision mechanism by a circularly polarized laser pulse, Phys. Rev. A 91 (2015) 043418.
[24] A.D. Bandrauk, K.J. Yuan, Molecular electron recollision dynamics in intense circularly polarized laser pulses, J. Phys. B: At. Mol. Opt. Phys. 51 (2018) 074001.
[25] X. Liu, X. Zhu, L. Li, Y. Li, Q. Zhang, P. Lan, P. Lu, Selection rules of high-order-harmonic generation: Symmetries of molecules and laser fields, Phys. Rev. A 94 (2016) 033410.
[26] X. Zhou, R. Lock, N. Wagner, W. Li, H.C. Kapteyn, M.M. Murnane, Elliptically polarized high-order harmonic emission from molecules in linearly polarized laser fields, Phys. Rev. Lett. 102 (2009) 073902.
[27] M. Qin, X. Zhu, Q. Zhang, W. Hong, P. Lu, Broadband large-ellipticity harmonic generation with polar molecules, Opt. Express 19 (2011) 25084–25092.
[28] S. Ramakrishna, P.A.J. Sherratt, A.D. Dutoi, T. Seideman, Origin and implication of ellipticity in high-order harmonic generation from aligned molecules, Phys. Rev. A 81 (2010) 021802(R).
[29] D.B. Milošević, W. Becker, High-order harmonic generation by bi-elliptical orthogonally polarized two-color fields, Phys. Rev. A 102 (2020) 023107.
[30] D. Habibović, D.B. Milošević, Ellipticity of high-order harmonics generated by aligned homonuclear diatomic molecules exposed to an orthogonal two-color laser field, Photonics 7 (2020) 110.
[31] X. Zhu, Q. Zhang, W. Hong, P. Lu, Z. Xu, Laser-polarization-dependent photoelectron angular distributions from polar molecules, Opt. Express 19 (2011) 24198–24209.
[32] G. Dixit, Á. Jiménez-Galán, L. Medišauskas, M. Ivanov, Control of the helicity of high-order harmonic radiation using bichromatic circularly polarized laser fields, Phys. Rev. A 98 (2018) 053402.
[33] D. Baykusheva, H.J. Wörner, Chiral discrimination through bielliptical high-harmonic spectroscopy, Phys. Rev. X 8 (2018) 031060.
[34] X. Zhang, X. Zhu, X. Liu, D. Wang, Q. Zhang, P. Lan, P. Lu, Ellipticity-tunable attosecond XUV pulse generation with a rotating bichromatic circularly polarized laser field, Opt. Lett. 42 (2017) 1027–1030.
[35] P. Huang, C. Hernández-García, J. Huang, P. Huang, C. Lu, L. Rego, D.D. Hickstein, J.L. Ellis, A. Jaron-Becker, A. Becker, S. Yang, C.G. Durfee, L. Plaja, H.C. Kapteyn, M.M. Murnane, A.H. Kung, M. Chen, Polarization control of isolated high-harmonic pulses, Nat. Photon. 12 (2018) 349–354.
[36] M. Qin, Y. Zeng, X. Zeng, Q. Liao, Enhancement of high-order harmonic generation due to the large gradient of the electric field amplitude, Appl. Sci. 9 (2019) 282.
[37] M. Peters, T.T. Nguyen-Dang, E. Charron, A. Keller, O. Atabek, Laser-induced electron diffraction: A tool for molecular orbital imaging, Phys. Rev. A 85 (2012) 053417.
[38] Y.J. Chen, L.B. Fu, J. Liu, Asymmetric molecular imaging through decoding odd-even high-order harmonics, Phys. Rev. Lett. 111 (2013) 073902.
[39] J. Javanainen, J.H. Eberly, Q. Su, Numerical simulations of multiphoton ionization and above-threshold electron spectra, Phys. Rev. A 38 (1988) 3430.
[40] M.D. Feit, J.A. Fleck, A. Steiger, Solution of the Schrödinger equation by a spectral method, J. Comput. Phys. 47 (1982) 412.
[41] K. Burnett, V.C. Reed, J. Cooper, P.L. Knight, Calculation of the background emitted during high-harmonic generation, Phys. Rev. A 45 (1992) 3347.
[42] S. Odžak, D.B. Milošević, Bicircular-laser-field-assisted electron-ion radiative recombination, Phys. Rev. A 92 (2015) 053416.